JOURNAL OF AIRCRAFT
Vol. 44, No. 4, July–August 2007

Hybrid Design for Aircraft Wind-Tunnel Testing Using Response Surface Methodologies

Drew Landman*
Old Dominion University, Norfolk, Virginia 23529
Jim Simpson†
Florida State University, Tallahassee, Florida 32310
Raffaello Mariani‡
Old Dominion University, Norfolk, Virginia 23529
Francisco Ortiz§
Florida State University, Tallahassee, Florida 32310
and
Colin Britcher¶
Old Dominion University, Norfolk, Virginia 23529

DOI: 10.2514/1.25914

A response surface methodology approach to wind-tunnel testing of high-performance aircraft is being investigated at the Langley Full-Scale Tunnel. An exploratory study was completed using a newly developed response surface methodology design in an effort to better characterize an aircraft's aerodynamic behavior while simultaneously reducing test time. This new design called a "nested face-centered design" was developed when classic designs were found to have inadequate prediction qualities over a cuboidal design space with factors at five levels. A 19% scale modified X-31 aircraft model was chosen for evaluation of the new response surface methodology design based on its nonlinear aerodynamic behavior at high angle of attack that is representative of modern fighter aircraft and due to a substantial preexisting data base. A five-level nested fractional factorial design, augmented with center points and axial points, produced regression models including pure cubic terms for the characteristic aerodynamic forces and moments over a cuboidal design space as a function of model position and control surface deflections. Model adequacy and uncertainty levels were described using robust statistical methods inherent to response surface methodology practice. Comparisons to baseline data and sample lateral–directional and longitudinal aerodynamic characteristics are given as validation of the new design.

Nomenclature

C_D = coefficient of drag
C_L = coefficient of lift
C_l = rolling moment coefficient
C_m = pitching moment coefficient
C_n = yawing moment coefficient
C_y = side force coefficient
q = dynamic pressure in pounds per square foot, psf
Y_1 = response from OFAT baseline run 1
Y_2 = response from OFAT baseline run 2
α = angle of attack in degrees, factor A
β = sideslip angle in degrees, factor B
δ_a = aileron deflection in degrees, factor D (right aileron trailing edge up positive, left aileron down)
δ_c = canard deflection in degrees, factor C (trailing edge up positive)
δ_r = rudder deflection in degrees, factor E (trailing edge left positive)
σ^2 = error variance (standard deviation squared)

Presented as Paper 7602 at the 2005 U.S. Air Force T & E Days, Nashville, TN, 5 December 2005–5 December 2009; received 15 June 2006; accepted for publication 19 March 2007.

*Associate Professor and Chief Engineer, Langley Full-Scale Tunnel (LFST), Department of Aerospace Engineering, 3750 Elkhorn Avenue. Senior Member AIAA.
†Associate Professor, Department of Industrial Engineering, 2525 Pottsdamer Street. Member AIAA.
‡Graduate Research Assistant, Department of Aerospace Engineering. Member AIAA.
§Graduate Research Assistant, Department of Industrial Engineering, 2525 Pottsdamer Street. Member AIAA.
¶Professor, Department of Aerospace Engineering, 3750 Elkhorn Avenue. Associate Fellow AIAA.

I. Introduction

THE process of wind-tunnel testing aircraft has the primary objective of characterizing the overall vehicle aerodynamic performance, stability, and control. Changes are made to independent variables (factors) such as angle of attack, sideslip angle, and control surface deflections while the six aerodynamic force and moment responses are recorded. The traditional approach to testing is to vary one factor at a time (OFAT), allowing all other factors to remain unchanged and presumed constant. Researchers will then pursue a course of experimentation aimed at sequentially modifying other variables to obtain data for a full mapping of the flight characteristics of interest. This approach requires that the entire system, which consists of the wind tunnel, the aircraft balance, and the data acquisition system, be completely stable throughout the entire test entry, which can last several weeks. Any errors that result from variations in the system are confounded with precision errors and are inseparable. In addition, if two or more inputs interact to affect a response, the OFAT experimentation approach will not easily detect these important contributions to response prediction and system understanding.

Proponents of design of experiments [DOE, of which response surface methodology (RSM) is a subset] have historically targeted engineers and scientists involved in manufacturing, chemical processing, the semiconductor industries, and agriculture. In recent

years, the aerospace community has begun formulating methods to exploit the benefits of DOE with regard to vehicle wind-tunnel testing [1–4]. The DOE approach differs from the OFAT approach because it is process oriented rather than task oriented. DOE methods approach an experiment by identifying all desired factors (independent variables) and all desired responses (outputs). Once all factors and responses are identified, a reduced run test matrix, also called a run schedule, is formulated. Executing this run schedule will provide statistically validated mathematical models of the responses in terms of the factors. The objective is to characterize the relationship between changes in system performance measures due to corresponding changes in system input factors. Bias errors due to uncontrolled or unknown system variations may be guarded against and uncertainty levels may be accurately estimated. Inherent to the DOE methodology is the construction of mathematical models detailing the response behavior being studied that are capable of predicting performance measures over the factor design space studied.

One of the challenges to using the DOE/RSM approach to wind-tunnel testing is that the researcher may have to choose limits to the experimental region before conducting the experiment. This may be acceptable over small ranges of sideslip and angle of attack or for a well-behaved region, but may not adequately represent the aerodynamic behavior over a region that includes aircraft stall and poststall behavior. When a new aircraft model is tested, the design space may be ill defined and exploration of the test envelope is routinely performed. In the current study, traditional OFAT-type pitch and yaw sweeps were conducted to define the limits of the entire design space and serve as a baseline comparison. A flexible RSM design was developed for use over subspaces encompassing the entire design space. Representative design spaces for both a high and low angle of attack range were then chosen and the hybrid RSM design was "scaled" to fit these regions.

Automated control surfaces are well suited to a fully randomized test program but are nearly always a source of increased set point error when compared to "fixed bracket" style surface setting. The RSM design presented here had to be robust to these inherent sources of error. This study focused on proving test methods and is not an all-inclusive aerodynamic characterization of the chosen aircraft. The overall goal of the methods presented here is to provide an efficient method of data collection for aircraft database and simulation development.

II. DOE and RSM in Wind-Tunnel Testing

DOE in its broadest sense is a process for planning an experiment so that appropriate data can be collected and analyzed by statistical methods, resulting in valid and objective conclusions [5,6]. A test matrix benefits from the three basic tenets of DOE: replication, randomization, and blocking. Randomization is the cornerstone of statistical methods in experimental design and requires that both the experimental factor level choices and the order of the runs are randomly determined. Statistical methods require that the error terms are normally and independently distributed random variables. Randomization also assists in averaging out the effects of extraneous factors that are sources of unknown and uncontrolled variation. Replication is the repetition of runs within the basic experiment. Replication of design points allows the researcher to determine an internal estimate of system noise and uncertainty. Blocking is a technique used to improve the precision with which comparisons among the factors of interests are made. Blocking is also used for reducing the variability transmitted through known but uncontrollable nuisance factors, that is, factors that may influence the experimental response but that are of no direct interest. For example, variations in wind-tunnel measurements are often encountered when comparing runs separated by overnight facility closings or shift changes. Assigning groups of runs to blocks helps separate the shift-to-shift variability that may occur due to atmospheric conditions, personnel changes, or from the force balance precision and other variances associated with data acquisition. RSM is a specialization within DOE and poses three general objectives in industrial experimentation: mapping a response surface over a particular region of interest, optimization of the responses, and selection of operating conditions to achieve specifications or customer requirements [7].

Analysis of the experimental data is performed using statistical hypothesis testing and regression model building so that the response values can be accurately estimated or predicted using empirical models. These models are usually low order polynomial functions of the input variables (factors), but with enough experimental runs of appropriate input settings in the test matrix, they can be of higher order. The model is evaluated for adequacy relative to additional model terms (lack-of-fit test). One of the greatest benefits in using DOE/RSM methods versus the traditional OFAT methods is the ability to include interaction terms in the analysis. The OFAT method only allows for one variable to be changed at a time, therefore it typically estimates main effects only. The DOE/RSM method allows, and partially requires, the change of more than one factor simultaneously, thus allowing for the discovery of interaction between variables. For example, OFAT can easily find the effect of sideslip angle on the rolling moment. DOE can efficiently estimate and predict the interaction effects that a change in sideslip angle and a deflection in aileron and rudder have on the rolling moment. The relative magnitudes of the coefficients in the regression model give direct feedback regarding the importance of the interaction effects to the overall responses.

Model design using a classical sequential DOE approach typically starts by allocating a subset of design points for building a linear model based on two-level factor settings. These factorial based models are then tested for fit, and if found inadequate they are augmented with additional points, yielding a quadratic model. Classical RSM second order designs focus on optimizing the design matrix for prediction variance and avoiding variable correlation over spherical or cuboidal experimental design spaces.

The advantage of using designed experiments in wind-tunnel testing has been explored in recent years and is gaining in popularity. The objective of this paper is to try to add to the existing science and not to necessarily provide a comprehensive treatise on the use of designed experiments. This paper then assumes that the reader has at least a fundamental understanding of the subject.

III. Exploratory Experiment

An exploratory experiment was conducted in the Langley Full-Scale Tunnel (LFST) to evaluate the potential of an RSM approach to aerodynamic characterization of a representative high-performance aircraft. A representative subset of actuated control surfaces was employed on an existing modified 19% scale model of the X-31 aircraft. Testing was conducted using a newly developed hybrid RSM design over a representative performance envelope range of angle of attack and sideslip.

A. Problem Statement

Aircraft wind-tunnel model designs have traditionally avoided remotely actuated control surfaces due to the added expense and inherent additional set point errors. Conversely, DOE and RSM methods are greatly aided by models of this type in the execution of a randomized test matrix. As such, control surfaces were actuated with remote devices for the aircraft used in this study.

The objective of the current study was to develop an efficient, cost effective, wind-tunnel test method to characterize the aerodynamic behavior of a typical high-performance aircraft. The wind-tunnel test procedure was limited to recording static force and moment measurements. The approach taken was to consider the development of a generic RSM model that could be scaled to work over subspaces of the entire design space defined by limits in the desired model attitude and control surface deflections. A requirement for the resulting empirically derived mathematical model was that it must have statistically based estimates of aerodynamic force and moment uncertainties and be robust to set point error. In addition, the model had to allow for interactions between factors and possess enough additional test run configurations (degrees of freedom) to estimate terms for pure cubic effects.

B. Experiment Details

Old Dominion University (ODU), working under a memorandum of agreement with NASA Langley Research Center, operates the LFST. The open-jet test section is semi-elliptical in cross section with a width of 18.29 m (60 ft) and a height of 9.14 m (30 ft). The ground board is 13 m (42.5 ft) wide by 16 m (52.3 ft) long and features a turntable with a diameter of 8.7 m (28.5 ft). Power is supplied by two 3 MW (4000 HP) electric motors driving two 11 m (36 ft) diameter four-bladed wooden fans. The current maximum speed is limited to approximately 130 kph (∼80 mph) in the test section [8].

The model support system used in this experiment consists of a large T-structure with a long rear-entry sting and is shown in Fig. 1. There were no boundary or flow corrections applied to the data as the objective of the study was simply to evaluate RSM test methods. It should be noted that baseline OFAT comparison data were taken using a slightly different support system with a shorter sting.

The aircraft model used in the study is a modified version of the 19% scale X-31 used by NASA Langley Research Center and is shown in Fig. 2 [9]. The model was unpowered and the vectored thrust paddles were removed; the canard, rudder, and outboard trailing-edge elevons (shown shaded gray in Fig. 2) were actuated by servo motors. The outboard elevons were moved differentially to act as ailerons: when the port surface was deflected upward, the starboard surface was deflected downward an equal amount. The control surface position tolerance was approximately ±3 deg, suitable only for nonprecision testing, like this exploratory project. The set up was fully automated; the attitude changes and control surface settings were commanded from the control room of the wind tunnel. The experiment was limited to a dynamic pressure of $q = 290$ Pa (6 psf) due to actuator power limitations at the extreme angles of attack.

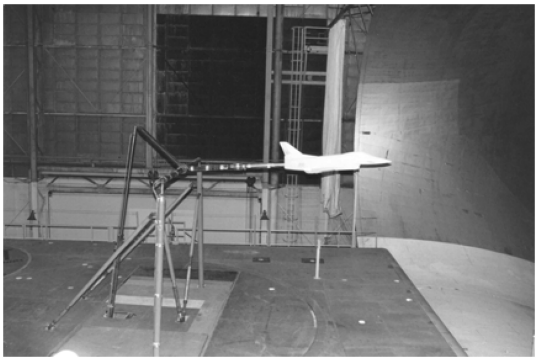

Fig. 1 X-31 model in LFST.

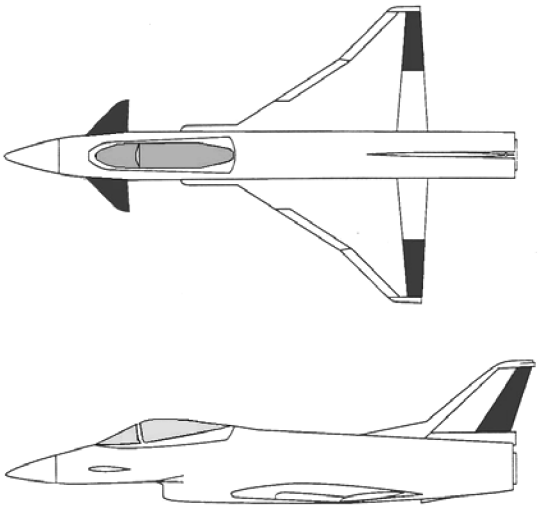

Fig. 2 Modified X-31 model with actuated control surfaces shown shaded in gray.

A 6 degrees of freedom FF-10MD internal strain gage balance (manufactured by Modern Machine and Tool, Hampton, Virginia) was used to collect force and moment data. A 16-bit PC-based data acquisition system was used to sample and reduce the balance data.

C. RSM Model Design Constraints

The aerodynamic behavior of high-performance aircraft is characterized by a prestall region at lower angles of attack where the lift curve slope is relatively constant, which is often called the linear region despite nonlinear responses. At higher angles of attack, due to the onset of stall, the lift curve becomes nonlinear. In the stall region, further effects are frequently observed, such as discontinuous response and hysteresis. In the poststall region, a more systematic behavior free of discontinuities and hysteresis is typically observed.

Experience with stability and control testing of aircraft models suggested the need for at least five levels of control surface deflection. Each surface would be deflected to ±50 and ±100% of the available throw in addition to the neutral setting. Current generation high-performance aircraft are capable of poststall maneuvers, extending the desirable range of angle of attack and sideslip. In the case of a new aircraft development program, the limits of the pitch envelope, for instance, may not be known, and hence an exploratory series of pitch polars at various sideslip angles will suffice to map the potential design space. This approach was adopted in the current investigation to establish a baseline data set. Lift curves using the baseline data are plotted in Fig. 3 for sideslip angles $0 < \beta < 16$ deg and an angle of attack range $-5 < \alpha < 70$ deg and were used to define the overall design space and the subspaces used for RSM model application. Following this exploratory phase, a subspace was denoted "RSM low" and chosen as representative of the low angle of attack, linear portion of the design space. Similarly an "RSM high" subspace was chosen in the stall/poststall region. Both are shown in Fig. 3. The character of the overall response

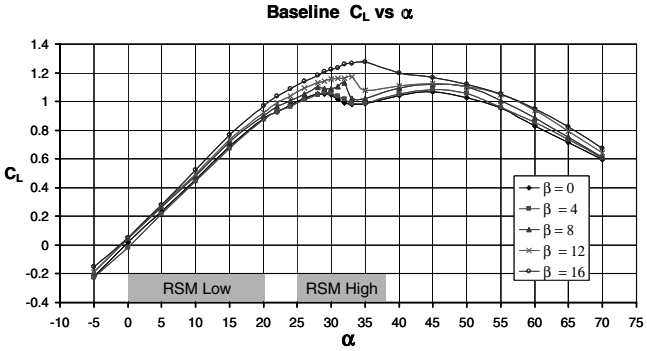

Fig. 3 Baseline lift curves at sideslip and identification of model subspaces.

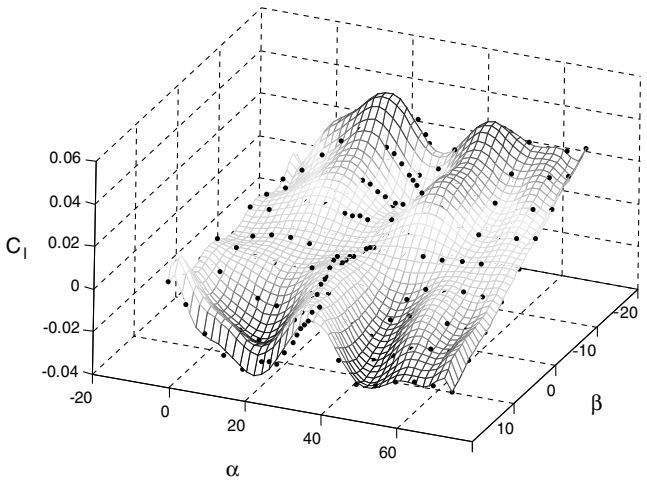

Fig. 4 Fitted surface for baseline rolling moment coefficient.

Table 1 Candidate nested FCD designs

No. of points	52	44	42	36	34
Inner factorial	1/2 fract	1/4 fract	1/2 fract	None	1/2 fract
Outer factorial	1/2 fract	1/2 fract	1/2 fract	1/2 fract	1/2 fract
Inner axials	Yes	Yes	No	Yes	No
Outer axials	Yes	Yes	Yes	Yes	Yes
Max. prediction variance (at a design point)	0.927	0.962	0.928	0.965	0.964
Ave. prediction variance	0.473	0.553	0.578	0.667	0.703
A-optimality	7.009	10.415	7.646	38.669	12.472
Max. VIF	9.0	15.4	9.9	65.9	19.0
Main effects and pure cubics	Yes	Yes	Yes	Yess	Yes

surfaces can be initially evaluated by surface fitting the baseline data. As an example, the baseline roll response is plotted in Fig. 4 using Kriging (MATLAB). Empirical models were desired which included as a minimum pure quadratic effects and two factor interactions, with enough degrees of freedom to evaluate the significance of pure cubic terms. No terms within the general model [Eq. (1)] are confounded. The models are of the form shown below where the βs are the empirically derived regression coefficients, the xs are the regressors, ε the error, and y represents a single response (e.g., lift coefficient or pitching moment coefficient).

$$y = \beta_0 + \sum_i \beta_i x_i + \sum_i \beta_{ii} x_i^2 + \sum \sum_{i \neq j} \beta_{ij} x_i x_j + \sum_i \beta_{iii} x_i^3 + \varepsilon$$
$$i = 1, 2, \ldots, k \tag{1}$$

D. Hybrid RSM Model: The Nested Face-Centered Design

A search for existing models that would fit the current criteria led to first reviewing the most popular RSM design with possible applicability, the classic central composite design (CCD). The CCD is well known for its run number efficiency and excellent prediction qualities. Designs identified as CCD can be classified by their characteristics: face centered, rotatable, and inscribed. The first step to selecting a CCD in a classical industrial experiment requires the experimenter to identify the *region of interest* and the *region of operability*. The region of interest is defined by the upper and lower limits of the factor settings that are of interest to the researcher, and the region of operability is defined by the upper and lower limits of the factor settings that can be safely achieved. In the current study these regions are coincident and suggest the face-centered CCD (FCD) as the best choice. Both the inscribed and the rotatable designs will lead to problems with extrapolation when predicting responses for factor settings at their extremes (corners). The limitation to the FCD is that it is a 3-level design. None of the standard CCDs meet all of the objectives of this study, which were to develop a model that predicts well over the cuboidal region, incorporate 5-level factor settings, and allow for potential joining of individual model subspaces [10,11].

The approach taken in this study was to leverage some of the advantages of the fractional factorial and the FCD with a new approach that would allow five levels. Equal increments in the control surface levels promoted the idea of a nested FCD anchored by a fractional factorial framework. The full nested FCD in two factors is shown graphically in Fig. 5. With more factors, the nested FCD geometry becomes hypercubes. The inner or outer cube could be fractionated (run some subset of all the hypercube vertices) such that the inner cube and outer cube could be alternate fractions. The points on the edge centers (axial points) in either cube could be omitted or retained. Five candidate designs were developed and are compared in Table 1. In addition to identifying the physical location of the design points, the table examines the issues of multicollinearity, prediction variance, and optimality. The variance inflation factor (VIF) is a metric used by regression model builders to quantify the degree of correlation between variables in the model. Generally a VIF less than 10 is desirable [7]. The scaled prediction variance allows the model builder to compare models by examining the relative uncertainty associated with response predictions from the model as a function of location in the design space on a per observation basis. Here we compare maximum and average scaled prediction variances for the five candidate designs, where it is in general desirable to achieve the lowest prediction variance. The design optimality criterion chosen in this study is A-optimality (a desire to maximize $X'X$), providing a direct comparison of variances associated with the regression model coefficients without including covariance between coefficients [7]. The 52 point design was chosen as that with the best qualities, however, the 42 point design represents a very close second choice. The point totals in Table 1 do not include center points, which were included in the design to obtain an internal estimate of pure experimental error. Upon the conclusion of this investigation, references were found to work by Draper in the 1960s on rotatable designs in three and four factors that benefited from a "nested" type approach [12,13].

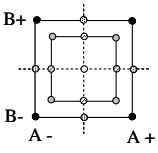

Fig. 5 Nested FCD in two factors.

E. Test Procedure

Each of two experiments (RSM low and RSM high) was conducted in single, continuous shifts on two consecutive days (no blocking required) and each test required approximately 5 h to complete. The test procedure that was followed was to always bring the aircraft attitude angles to a value of zero between successive run points to avoid aerodynamic hysteresis. The chosen factor levels for the two experiments are given in Table 2 and the complete randomized test matrix for RSM low is given in Table 3. The bold points of Table 3 correspond to the center points of the design; three center points were added to each of the subspace designs.

IV. Analysis of Results

The data collected were analyzed using least-squares estimation with the aid of Design Expert™, a commercially available program. First, a tentative regression model with all factors was developed for each of the responses up to and including pure cubic terms. The purpose of this analysis is to determine which factors, multifactor interactions, and higher order polynomial terms affect each response in order to develop an empirical model that accurately predicts

Table 2 Factor limits (all values in degrees with center levels in bold)

	Factor levels					Subspace
α	0	5	**10**	15	20	RSM low
	25	28	**31**	34	37	RSM ligh
β	−10	−5	**0**	5	10	Both
δ_c	−30	−15	**0**	15	30	Both
δ_a	−30	−15	**0**	15	30	Both
δ_r	−20	−10	**0**	10	20	Both

Table 3 RSM low nested FCD design test matrix (center runs shown as bold)

Run	α	β	δ_c	δ_a	δ_r	Run	α	β	δ_c	δ_a	δ_r
1	5	5	15	15	−10	29	5	−5	−15	15	−10
2	0	−10	30	30	−20	30	5	5	15	−15	10
3	5	5	−15	−15	−10	31	10	10	0	0	0
4	15	−5	−15	−15	−10	32	5	0	0	0	0
5	5	−5	−15	−15	10	33	10	0	15	0	0
6	**10**	**0**	**0**	**0**	**0**	**34**	**10**	**0**	**0**	**0**	**0**
7	15	−5	15	−15	10	35	20	−10	30	−30	−20
8	10	0	0	0	−20	36	10	0	30	0	0
9	0	10	−30	−30	20	37	0	10	−30	30	−20
10	15	5	−15	−15	10	38	10	0	0	0	20
11	10	0	0	0	10	**39**	**10**	**0**	**0**	**0**	**0**
12	20	10	−30	−30	−20	40	5	−5	15	15	10
13	20	10	30	−30	20	41	15	0	0	0	0
14	10	5	0	0	0	42	10	−5	0	0	0
15	0	10	30	−30	−20	43	20	0	0	0	0
16	5	−5	15	−15	−10	44	15	5	15	−15	−10
17	15	5	15	15	10	45	5	5	−15	15	10
18	15	−5	−15	15	10	46	20	10	−30	30	20
19	10	0	−30	0	0	47	0	−10	−30	30	20
20	20	10	30	30	−20	48	10	0	0	−15	0
21	20	−10	−30	−30	20	49	0	−10	−30	−30	−20
22	20	−10	30	30	20	50	10	0	0	30	0
23	20	−10	−30	30	−20	51	0	10	30	30	20
24	10	0	0	15	0	52	0	−10	30	−30	20
25	0	0	0	0	0	53	10	0	0	−30	0
26	10	0	0	0	−10	54	10	0	−15	0	0
27	15	5	−15	15	−10	55	10	−10	0	0	0
28	15	−5	15	15	−10						

Table 4 Analysis of variance table for C_L

ANOVA for C_L response surface RSM low subspace					
Source	Sum of squares	DF	Mean square	F value	Prob > F
Model	4.335542	8	0.541943	4628.06	<0.0001
A	0.534207	1	0.534207	4562.00	<0.0001
B	6.26*E*-06	1	6.26*E*-06	0.05	0.8182
C	0.027679	1	0.027679	236.37	<0.0001
D	7.66*E*-05	1	7.66*E*-05	0.65	0.4227
A^2	0.000938	1	0.000938	8.01	0.0069
C^2	0.003358	1	0.003358	28.68	<0.0001
BD	0.005391	1	0.005391	46.03	<0.0001
A^3	0.002003	1	0.002003	17.10	0.0001
Residual	0.005387	46	0.000117	——	——
Lack of fit	0.005288	44	0.00012	2.44	0.3343
Pure error	9.87*E*-05	2	4.93*E*-05	——	——
Cor. total	4.340928	54	——	——	——
Factor labeling key					
Label	A	B	C	D	E
Factor	α	β	δ_c	δ_a	δ_r

response values for any factor settings between the low and the high levels. Using the mean squares for each factor versus the mean square for error, an F-test is performed at a 5% level of significance. The model is consequently refined by dropping insignificant factors, and a table of significance, called the analysis of variance (ANOVA) table, is then computed. A sample ANOVA table is included as Table 4 for the lift response of the low angle of attack subspace.

The model is considered tentative until the model assumptions of normally, independently distributed error with constant variance are tested. The model residuals, the actual model response values subtracted from the regression model predicted response values, are estimates of the true model errors. Normality is evaluated by plotting rank ordered observations against their observed cumulative frequency and is somewhat subjective. No problems were encountered with normality in this study. Plotting residuals versus predicted values provides a check for constant variance, a fundamental requirement to the model fitting. Finally, plotting residuals versus run checks for systematic variation over time that may mean the assumption of independence has been violated. No significant structure in the residuals should be observed and they should remain within an upper and a lower limit of three studentized units. A representative sample of residual diagnostic plots from the lift coefficient of the RSM low subspace is included in Fig. 6. Having passed the diagnostic checks, a regression model for each of the aerodynamic coefficient responses was now available. Table 5 provides a summary of each of the significant terms from the regression models for each of the responses. Note that the term

Table 5 Significant model terms

	RSM high						RSM low					
Term	C_Y	C_l	C_m	C_n	C_L	C_D	C_Y	C_l	C_m	C_n	C_L	C_D
A	×	×	×	×	×	×	×	×	×	×	×	×
B	×	×		×	×	×	×	×	×	×	×	×
C	×		×		×	×	×	×	×	×	×	×
D		×		×	×		×	×	×	×	×	×
E	×	×	×	×	×	×	×	×		×	×	×
A^2			×		×			×			×	×
B^2	×	×			×	×	×	×				
C^2			×						×		×	×
D^2		×					×	×				×
E^2					×	×	×	×		×	×	
AB	×	×		×			×	×		×		
AC						×			×			×
AD				×				×		×		
AE				×								
BC	×						×	×		×		
BD									×		×	
BE								×				×
CD								×				
CE												×
DE				×			×			×		
A^3			×		×	×					×	×
B^3	×	×					×	×				
C^3									×			×
D^3							×	×				
E^3							×	×		×	×	

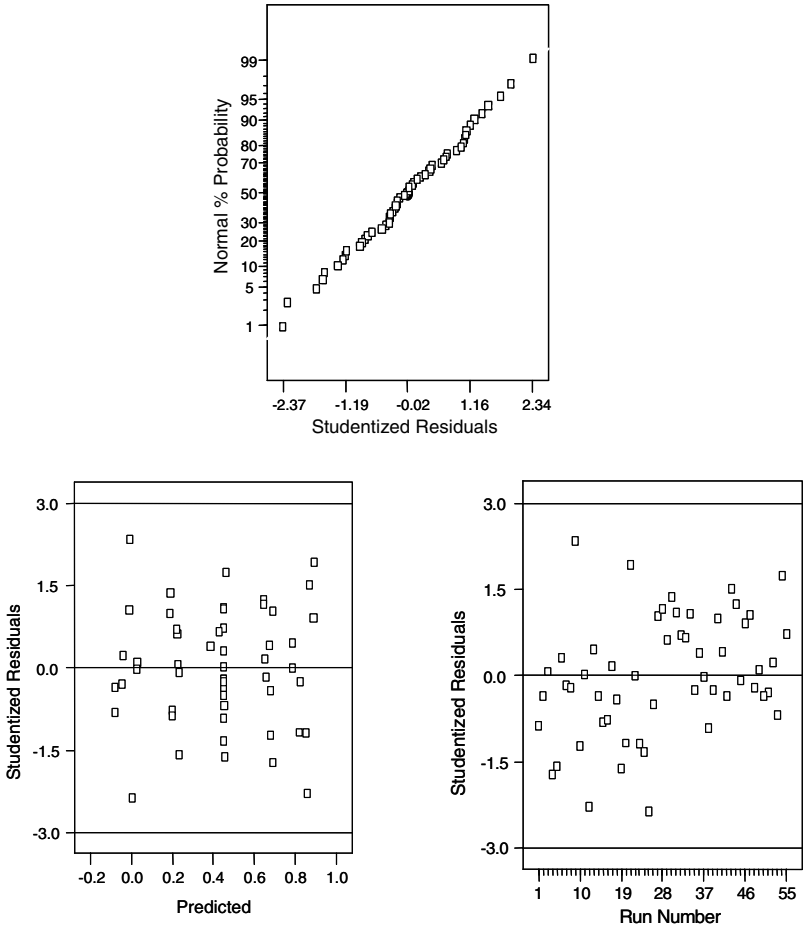

Fig. 6 Diagnostic residual plots for lift coefficient of RSM low subspace.

definitions are given under the nomenclature section and that model hierarchy was maintained [5,6]. A 95% confidence half-interval on the response is computed by taking the t statistic times the square root of the mean square for error (shown under the heading of "residual" in the example of Table 4) [5–7].

V. Results and Discussion

The focus of this study has been to show that the nested FCD design is a flexible, efficient method for aerodynamic characterization over design subspaces. In this section specific comparisons to baseline data are used to informally validate the models and show that they well represent the data. In addition, representative plots derived from the regression models are presented to illustrate their utility at providing traditional aircraft stability and control data.

Two (OFAT) lift curves were generated on two different days using the X-31 model with control surfaces mechanically fixed at zero deflection. A 95% *precision* confidence interval was computed using an estimate of variance calculated from the sum of root mean square differences between the two baseline run responses and is reflected in the error bars of all data presented as "baseline." The calculation for the variance estimate is given in Eq. (2). The confidence half-interval is then represented as the t statistic times the square root of the variance estimate. Of course, all RSM based confidence intervals necessarily include the effects of set point error from all the control surfaces and are larger in magnitude in comparison.

$$\hat{\sigma}^2_{\text{baseline}} = \frac{1}{N-1}\sum_{i=1}^{N}(Y_{1_i} - Y_{2_i})^2 \tag{2}$$

Representative longitudinal characteristics are explored first. The lift curve of Fig. 7 shows the superposition of results from the two RSM experiments and the baseline (OFAT) data. Point symbols were omitted from the RSM model as the response function is continuous. Error bars are provided at discrete points for interpretation. This figure illustrates that the FCD predicted well both over the 20 deg range at low angle of attack and over the 8 deg range at high angle of attack. Graphically, we see that the pure cubic dependency on angle of attack is much greater in the high range versus the low range as expected and that the model is able to capture the character of the response. The same data sets are used in the drag polar of Fig. 8, with similar prediction results. Sample lateral characteristics are explored in Fig. 9 where the rolling moment versus sideslip angle is compared to the baseline data using the RSM high model, again with good agreement. In all cases predictions from the model are in agreement with the baseline data as can be seen by the overlapping error bars. Although this is an informal comparison it serves to show the potential of the method, the goal in this study. A formal error budget could be specified and a precision actuated (or fixed control bracket) model built to comply with strict precision goals.

Rudder effectiveness is explored in Fig. 10 for two different angles of attack. The regression model for yawing moment was used to provide predictions for five sideslip angles with the rudder deflected 20 deg and ailerons and canard set neutral. At first glance the plot appears to show that there may be some loss of rudder authority at the high angles of attack, but upon closer inspection it is seen that the confidence intervals of the 10 deg responses always contain the 35 deg responses so that we cannot justify this hypothesis. Although the uncertainty levels are relatively high in this exploratory experiment, the point is being made that traditional OFAT testing often cannot easily offer a robust estimate for the error shown, where here all control surface set point errors are accounted for simultaneously.

Canard control effectiveness is illustrated in Fig. 11. The increment in pitching moment is evaluated as a function of canard

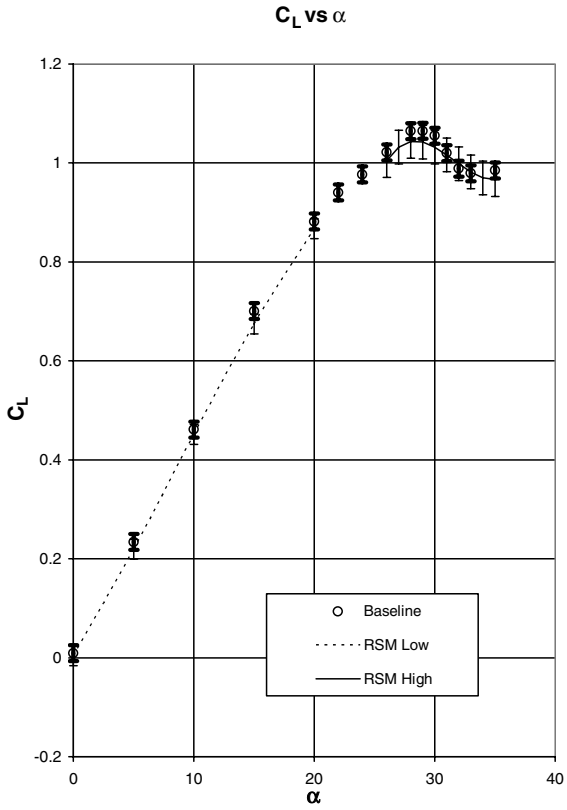

Fig. 7 Comparison of baseline lift curve to RSM model estimates (all control surfaces at center level).

deflection over four angles of attack using evaluations of the regression model at five values of canard deflection. Again, taking into account the error estimates, it is seen that the canard control power is relatively unchanged over the pitch range shown which is a result corroborated by [9]. Error bars are provided for the data of the highest and lowest angles of attack.

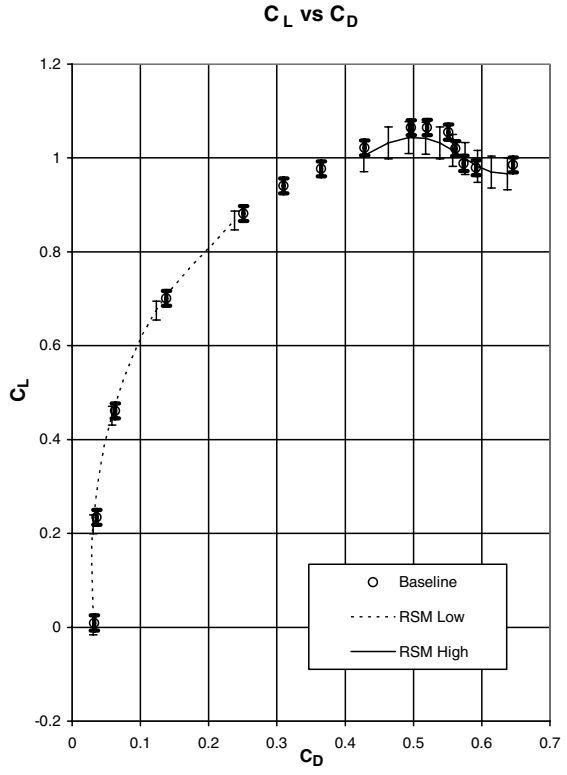

Fig. 8 Comparison of baseline drag polar to RSM model estimates (all control surfaces at center level).

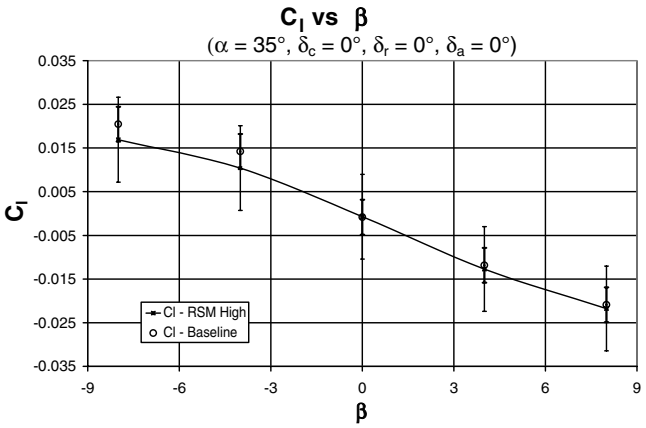

Fig. 9 Comparison of baseline to RSM high estimates, rolling moment versus sideslip.

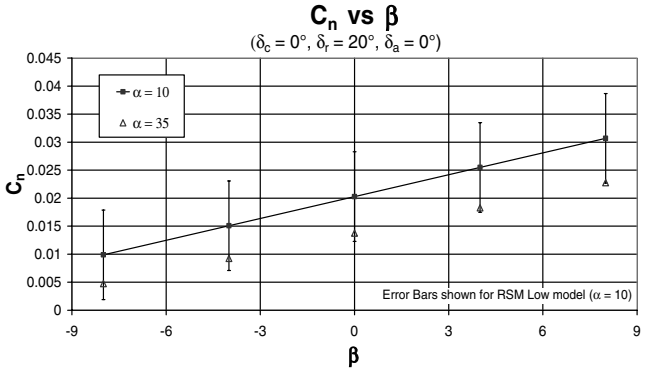

Fig. 10 RSM model estimates of rudder effectiveness.

Aileron control power was evaluated using the regression models for rolling and yawing moments at five deflections for two angles of attack and is shown in Fig. 12. Here it is clearly shown that roll control is more limited at 35 deg than at 10 deg, while the resulting yawing moment response is relatively constant. Confidence is gained in this result after reviewing the uncertainty bounds.

The representative control power plots are one example of classical test data results available using the RSM methodology. Interactions represent potential new results afforded by employing the RSM method. As a simple example, consider the effect that ailerons will have on lift as the aircraft is yawed. Figure 13 is a three-dimensional plot representing the lift response surface at an angle of

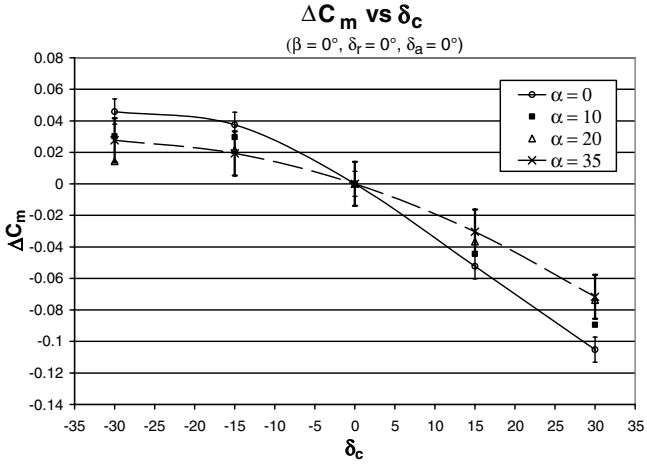

Fig. 11 RSM model estimates of canard effectiveness.

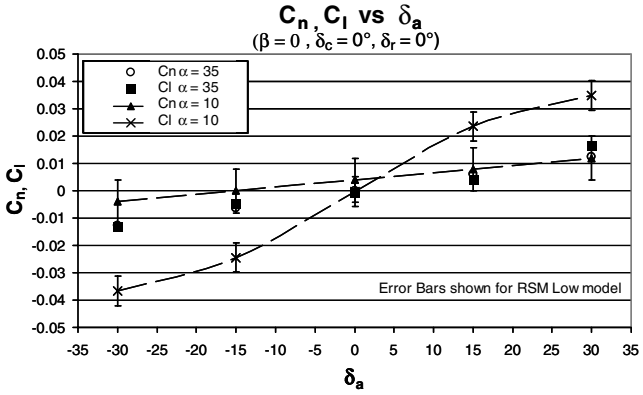

Fig. 12 RSM model estimates of aileron effectiveness.

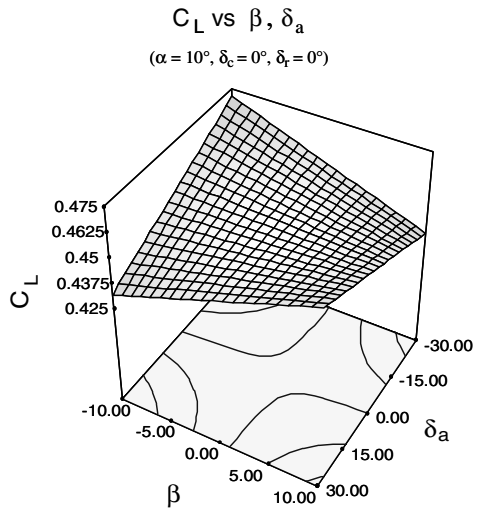

Fig. 13 Lift coefficient response surface, an example of interaction.

attack of 10 deg. Here the canard and rudder are centered while the effect of aileron sweeps of ± 30 deg can be evaluated. Note that the lift coefficient at sideslip depends on the direction of aileron deflection—a simple interaction. This intuitive example is meant to illustrate the power of the method at unearthing more complex interactions. Consider now the trailing edge of a flying wing transport aircraft, populated with 10 adjacent control surfaces. Interactions now become much more difficult and time consuming to obtain using traditional OFAT methods yet the DOE approach will inherently identify the interactions as part of the test methodology [14].

VI. Conclusions

The nested FCD design proved to be effective at high-performance aircraft aerodynamic characterization over two representative design subspaces. Subsequent use of this experimental approach can provide an aerodynamic database and is suitable for computer based flight simulation. Because the set point error inherent to the control surface actuators is "averaged" over the entire experiment, effects are attenuated which may suggest the use of less costly wind-tunnel models for new aircraft development. Conversely, the RSM model design should prove effective in high fidelity, precision testing environments with well-defined error budgets and can be scaled appropriately to meet the needs of the researcher.

References

[1] DeLoach, R., "Tactical Defenses Against Systematic Variation in Wind Tunnel Testing," AIAA Paper 2002-0885, 2002.

[2] Landman, D., Simpson, J., Sumner, T., and Hall, B., "Use of Designed Experiments in Wind Tunnel Testing of Performance Automobiles," SAE 2002 Transactions: Journal of Passenger Cars, 2002, pp. 2339–2346.

[3] DeLoach, R., and Berrier, B. L., "Productivity and Quality Enhancements in a Configuration Aerodynamics Test Using the Modern Design of Experiments," AIAA Paper 2004-1145, 2004.

[4] DeLoach, R., "MDOE Perspectives on Wind Tunnel Testing Objectives," AIAA Paper 2002-2796, 2004.

[5] Montgomery, D. C., *Design and Analysis of Experiments*, 5th ed., Wiley, New York, 2001.

[6] Box, G., Hunter, J. S., and Hunter, W., *Statistics for Experimenters: An Introduction to Design, Data Analysis, and Model Building*, Wiley, New York, 1978.

[7] Myers, R. H., and Montgomery, D. C., *Response Surface Methodology*, 2nd ed., Wiley, New York, 2002.

[8] Britcher, C. P., and Landman, D., "From the 30×60 to the Langley Full-Scale Tunnel," AIAA Paper 98-0145, 1998.

[9] Banks, D. M., and Paulson, J., Jr., "Low-Speed Longitudinal and Lateral-Directional Aerodynamic Characteristics of the X-31 Configuration," NASA TM-4351, 1992.

[10] DeLoach, R., and Erickson, G. E., "Low-Order Response Surface Modeling of Wind Tunnel Data over Truncated Inference Subspaces," AIAA Paper 2003-456, 2003.

[11] Morelli, E. A., and Deloach, R., "Wind Tunnel Database Development Using Modern Experiment Design and Multivariate Orthogonal Functions," AIAA Paper 2003-653, 2003.

[12] Draper, N. R., "Third Order Rotatable Designs in Three Factors," *Technometrics*, Vol. 4, No. 2, 1962, pp. 219–234.

[13] Draper, N. R., "A Third Order Rotatable Design in Four Dimensions," *Annals of Mathematical Statistics*, Vol. 31, No. 4, 1960, pp. 875–877.

[14] Landman, D., Simpson, J., Vicroy, D., and Parker, P., "Efficient Methods for Complex Aircraft Configuration Aerodynamic Characterization Using Response Surface Methodologies," AIAA Paper 2006-922, 2006.